Control of shunt-wound motors with DC/DC converters using the pole placement technique

Nadheer Abdulridha Shalash, Wameedh Riyadh Abdul-Adheem, Yasir Khaldoon Abdul Jabbar
Department of Electrical Power Techniques Engineering, AL_Ma'moon University College, Baghdad, Iraq

Article Info

Article history:

Received Dec 20, 2020
Revised Jan 4, 2022
Accepted Jan 15, 2022

Keywords:

Boost converter
Buck converter
DC shunt motor
PI controller
Pole placement control

ABSTRACT

Many techniques have been developed for the speed manipulation of shunt-wound direct current motors (SWDCMs) established based on armature and field control. The current research proposes a controller based on the pole placement (PP) control technique and compares it with a proportional integral (PI) controller for trajectory speed control of SWDCM with uncertainty. The circuit of the DC/DC converters energizes the DC motor. The responses are analyzed according to the dynamic mathematical model of the implemented controllers and the model of the DC/DC converters. Comparison of the motor dynamical response of the conventional PI and proposed PP controllers indicates that the PP controller exhibits improved performance in terms of rise time and steady-state error.

Corresponding Author:

Nadheer Abdulridha Shalash
Department of Electrical Power Techniques Engineering, AL_Ma'moon University College
Baghdad, Iraq
Email: nadheer.a.shalash@almamonuc.edu.iq

1. INTRODUCTION

The DC motors are utilized in many real-world applications, such as cement production, steel factories, cutters, winches, hoists, fabric devices, grinding engines, welding machine, winch rollers, tool machinery, fans, drilling, automobiles, and robotics [1]–[4]. Direct current (DC) motors are the most preferred among various kinds of electric motors because they easily meet motion requirements. However, reducing the energy utilization of electric-motor-driven systems with high power remains problematic and unsolved.

Shunt-wound DC motors (SWDCMs) are generally used in applications with high demands for load torque or power [1]. SWDCMs are broadly utilized in many manufacturing applications in which a rotational system needs to have a constant speed to perform particular functions and purposes. Notable examples include electric automobiles, rolling and robotic manipulators, and cutting and threading steel mills due to the need for accurate control features [5]. A technique to integrate the dynamics of fractional order into an available control system of a DC via an inner proportional integral (PI) or proportional integral derivative (PID) controller was developed in [6]. A novel adaptive speed path tracking control system for nonlinear SWDCMs subjected to changeable load torque and parametric uncertainty was proposed in [7]. A smart speed controller for SWDCMs on the basis of the nonlinear autoregressive method was presented in [5]. A contrast of a closed-loop DC/DC converter on a solar basis that utilizes SWDCM force PID and fuzzy logic control was introduced in [8]. The full-state feedback (FSF) or pole placement (PP) technique is a means of utilizing feedback control theory to situate plant closed-loop poles in prearranged places on the s-plane [1]. Situating poles are desirable because the site of poles is a straightforward match of system eigenvalues, which organize the properties of the system response. The system should be regarded as controllable to apply this technique. Moreover, in [9], optimal FSF for separately excited and series-excited motor configurations with a buck converter was considered. The design and implementation of a controller for adaptive feedback linearization in an SWDCM were introduced in [10]. In [11], three dissimilar techniques, namely, input–output linearization, feedback linearization, and fuzzy logic control, for the nonlinear control design of SWDCM velocity were assessed.

The current study uses the PP technique to design an angular speed controller for an SWDCM with uncertainty. The focus of this work is to develop a control system with high-speed tracking accuracy and response features of SWDCM with uncertainty. The proposed controller can considerably improve the control performance of the motor. In the design of the PP controller, we consider the model of the DC/DC converter. Many studies have been conducted on converter models, such as buck, boost, and buck–boost converters. In this study, however, the buck and boost models are considered drivers for SWDCMs. The effectiveness of the proposed controller is verified by comparing its simulation results with those of a straight PI controller.

The remainder of the paper is structured as follows. Section 2 tackles the modeling of the DC motor and the models of DC/DC converters. Moreover, this section presents and discusses the PI-controlled chopper structure with the DC motor. Section 3 addresses the results of the numerical simulation for the proposed PP technique and conventional PI controller by utilizing the MATLAB®/Simulink® package. Section 4 provides the conclusions.

2. RESEARCH METHOD

2.1. Modeling and dynamics

2.1.1. Shunt-wound DC motor (SWDCM)

The objective of developing the mathematical model lies in associating the voltage that is applied to the armature to motor velocity. Two differential equations are developed in consideration of the system's mechanical and electrical properties [10]. Figure 1 illustrates the corresponding electrical circuit of SWDCM. The details of the signals and parameters cited in the equations are presented as the voltage supply (V_a) along the armature coil. We describe the armature coil to be electrically equivalent to inductance (L_a) in a series with resistance (R_a). The field circuit linked along the armature contains inductance and resistance values L_f and R_f, respectively. ω, B, and J respectively represent the rotary velocity, coefficient of viscous friction, and instant of inertia connected to the load and motor together [11]. The electrical coil rotation generates induced voltage e_b via field winding stable flux lines [2]. Utilizing Kirchoff's voltage law produces the dynamic equations of the equivalent circuit of the SWDCM method around the electrical loop [2]. By achieving energy balance in the method, the total of motor torques equals zero [3], and (1)-(3) are obtained.

$$v_f = R_f i_f + L_f \frac{di_f}{dt} \quad (1)$$

$$v_a - e_a = R_a i_a + L_a \frac{di_a}{dt} \quad (2)$$

$$T_e = J\frac{d\omega}{dt} + T_L + B\omega \quad (3)$$

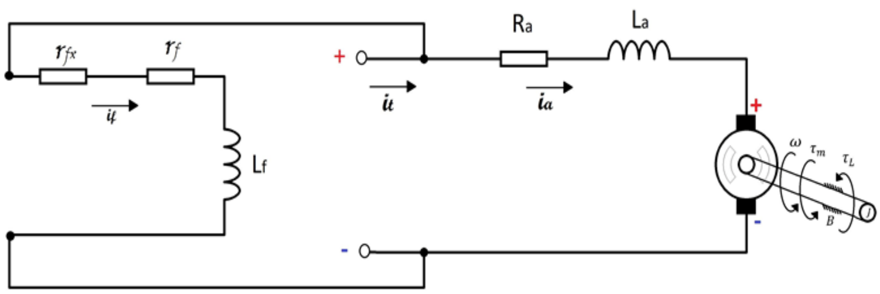

Figure 1. Schematic of SWDCM [1], [12]

2.1.2. Buck converter

Figure 2 displays a diagram of the buck converter circuit. The transistor functions with a stable frequency in period T and on time to period time percentage or duty ratio (d) [13]. The current of the inductor is presumed to be constant [14]. The relation between the duty ratio and stable output voltage can be achieved by equating the volt-seconds of the positive and negative inductors in a switching series. The volt-seconds should stabilize in a fixed state process.

$$(V_i - V)d\tau = V(1 - D) \tag{4}$$

$$V = DV_i \tag{5}$$

Given that the value of D is between 0 and 1, the output voltage of the converter should be lower than or equivalent to the input voltage.

The typical condition of the converter control system is to keep the output voltage steady regardless of the differences in the voltage of DC source V_i and the current of the load. With respect to the fixed state equation of the output voltage, V_i is independent of the load conditions. However, alterations in load influence the output voltage in a transitory manner and may result in essential deviations from the fixed state level. Moreover, circuit losses in a practical system present a dependency of the output voltage on the current of the fixed state load, which should be balanced by the control system. The converter model of state and space can be expressed as the following equations [9], [14]:

$$\frac{di_L}{dt} = \left(\frac{1}{L}\right)(DV_i - V_a - R_L i_L) \tag{6}$$

$$\frac{dV_c}{dt} = \left(\frac{1}{C}\right)(i_L - i_a) \tag{7}$$

$$V_a = V_c + R_c(i_L - i_a) \tag{8}$$

where V_i(V) represents the input voltage, i_a(A) describes the current of the armature, $R_L(\Omega)$ represents the resistance of the inductor, L(H) denotes the buck inductor inductance, C(F) refers to the capacitance of the capacitor of the buck converter, and $R_C(\Omega)$ stands for the resistance of equivalent series. Table 1 shows the buck converter parameters used in the study.

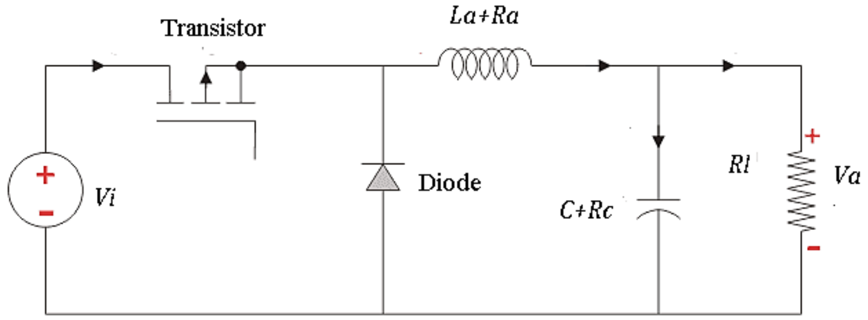

Figure 2. Buck converter circuit diagram [15]

Table 1. Buck converter parameters

Parameter	Value
$R_L(\Omega)$	0.017
L(mH)	1.5
$R_C(\Omega)$	0.25
C(μF)	9,400

2.1.3. Boost converter

Figure 3 depicts the circuit diagram of the boost converter. We assume that the semi-conductors are ideal. Accordingly, the blocking and conduction states are applied without any absolute loss of time. The diode is inversely polarized when the transistor is in the ON state [11]. Therefore, the energy does not flow to the driven system from source V_i. Moreover, the diode is forwardly polarized when the state of the transistor is OFF. This condition permits the energy to flow to the load [15], [16].

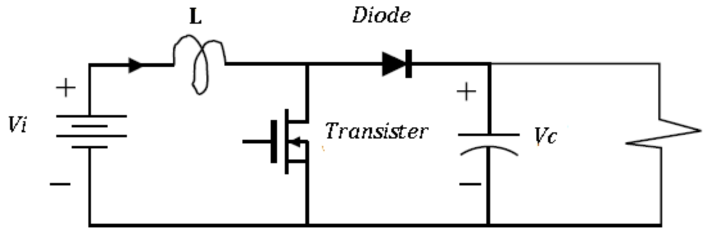

Figure 3. Boost converter circuit diagram [17]

The boost converter modeling equations are designed according to the following [18]–[20]:

$$L\,\frac{di_L}{dt} = V_i - (1-D)V_c, \tag{9}$$

$$C\,\frac{dV_c}{dt} = i_L(1-D) - i_a, \tag{10}$$

where i_L represents the current of the inductor, V_c denotes the voltage of the capacitor, and i_a stands for the current of the armature. Pointing to the DC/DC converter, L and C signify the inductance and capacitance of the converter, respectively. V_i signifies the DC input voltage, and D signifies the duty ratio standing for the ratio of the switching cycle in a period. With regard to the DC motor, the parameters of the boost converter system design are V_i=10 V, $L = 16\times\ 10^{-3}$ H, and $C = 57\times10^{6}$ F.

2.2. The proposed PP controller

In this section, The PP controller was devised with a buck/boost converter similar to a blocked round element of the control approach to preserve the velocity of SWDCM, as shown in Figure 4. The control law of the proposed PP controller can be expressed as (11):

$$D = \omega_{ref} - Kx + k_6\int e_\omega dt, \tag{11}$$

where $x = [i_L v_C i_\alpha \omega i_f]$ is the state vector of the complete model, which is composed of SWDCM and the DC/DC converter; $e_\omega = \omega_{ref} - \omega$ represents the speed tracking error; and $[\ K\ k_6]$ is the gain vector of the proposed PP controller.

On the basis of the system description provided in this section, the evaluated state-feedback gain vectors for boost and buck are $K_{boost} = [\ k_1\ k_2\ k_3\ k_4\ k_5\ k_6] = [0.3\ \ 2.9\ \ 0.13\ \ 79.21\ \ 141.21\ \ 20]$ and $K_{buck} = [\ k_1\ k_2\ k_3\ k_4\ k_5\ k_6] = [1.73\ \ 0.68\ \ 0.71\ \ 41.88\ \ 654.21\ \ 100]$, respectively. For comparison, a classical PI controller was devised with the buck/boost converter and feedback of the control strategy to preserve the velocity of SWDCM, as shown in Figure 5 [21]–[23]. The control law of this case is presented as (12):

$$D = K_1 e_\omega + k_2\int e_\omega dt \tag{12}$$

where $e_\omega = \omega_{ref} - \omega$ represents the speed tracking error and $[\ k_1\ k_2]$ denotes the gain vector of the proposed PI controller.

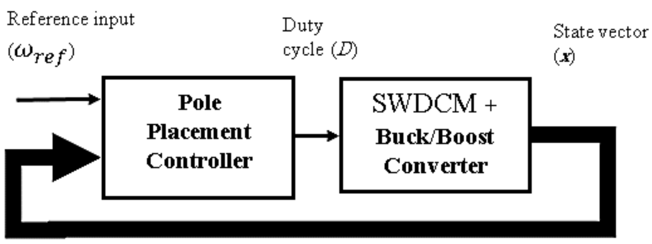

Figure 4. Block diagram of the proposed pole placement controller

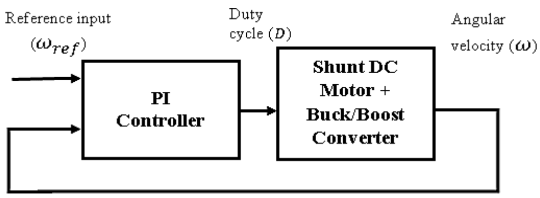

Figure 5. Block diagram of the conventional PI controller

On the basis of the system description provided in this section, the evaluated state-feedback gain vectors for boost and buck are $K_{boost} = [k_1\ k_2] = [0.0208\ 0.0005]\ and\ K_{buck} = [k_1\ k_2] = [0.016\ 0.0017]$ respectively. Other controllers can be utilized, such as the normalized fuzzy logic controller which is presented in [24] and this controller can be optimized by using the enhanced particle swarm optimization algorithm presented in [25].

2.3. Numerical simulation

We performed a simulation to apply the recommended control design in practice. We examined the DC motor velocity control that utilizes PI and PP controllers. The recommended control designs were simulated and evaluated in the simulation setting of the buck and boost converters motivating SWDCM. Figures 6(a), 6(b) and 6(c) present the equivalent simulation blocks.

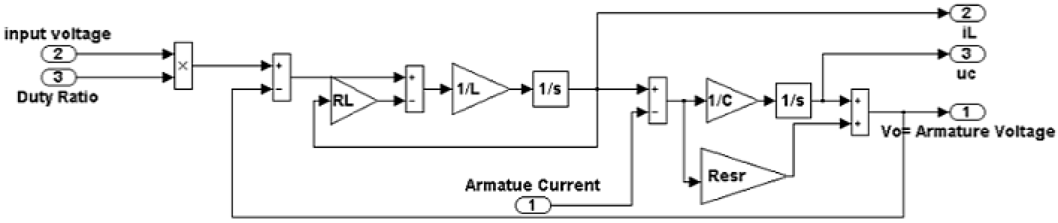

(a)

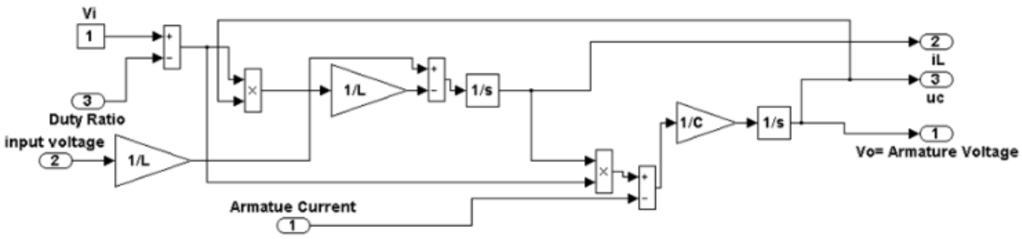

(b)

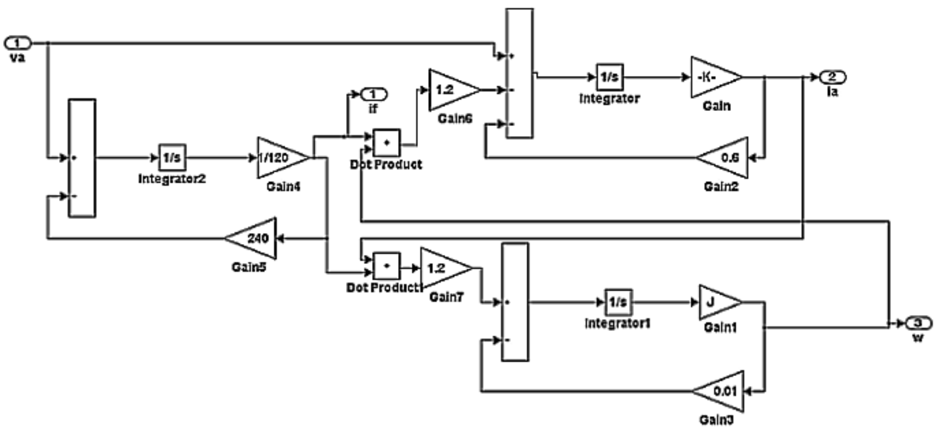

(c)

Figure 6. Block diagram of MATLAB®/Simulink® (a) buck convertor, (b) boost convertor, and (c) SWDCM

3. RESULTS AND DISCUSSION

In this section, the results of the numerical simulation for the proposed PP technique and conventional PI controller supporting the types of DC/DC converters are presented in Figures 7 to 15. When a boost converter is utilized, the feedback controller presents a rise time (t_r) that equals 7.2 s in comparison with the PI controller, which has t_r=18.9 s as shown in Figures 7 and 10. Furthermore, the steady-state error e_{ss}=0.2% at J=1 compared with e_{ss}=2.84% at J=0.9 for the PI controller as shown in Figures 11 and 13.

This progress in time characteristics was due to the use of multiple states in building the signal of the feedback control law. The only limitation of the proposed controller is the chattering that emerges from the field current (i_f) of the PP controller as shown in Figure 9 in comparison with the field current (i_f) of the PI controller as shown in Figure 12. However, the chattering decreased with the decrease in inertia J. Chattering in the field current (i_f) related to the PP controller was observed in the armature current (i_a) as well as shown in Figure 8 compared with that of the PI controller as shown in Figure 11.

The improvement in time characteristics was observed with the utilization of the buck converter as shown in Table 2 and Figures 13 and 16 for PP and PI controllers, respectively). Chattering was absent from field and armature currents (i_f) and (i_a) as shown in Figures 13, 14, 17, and 18, indicating further progress in utilizing the proposed PP controller.

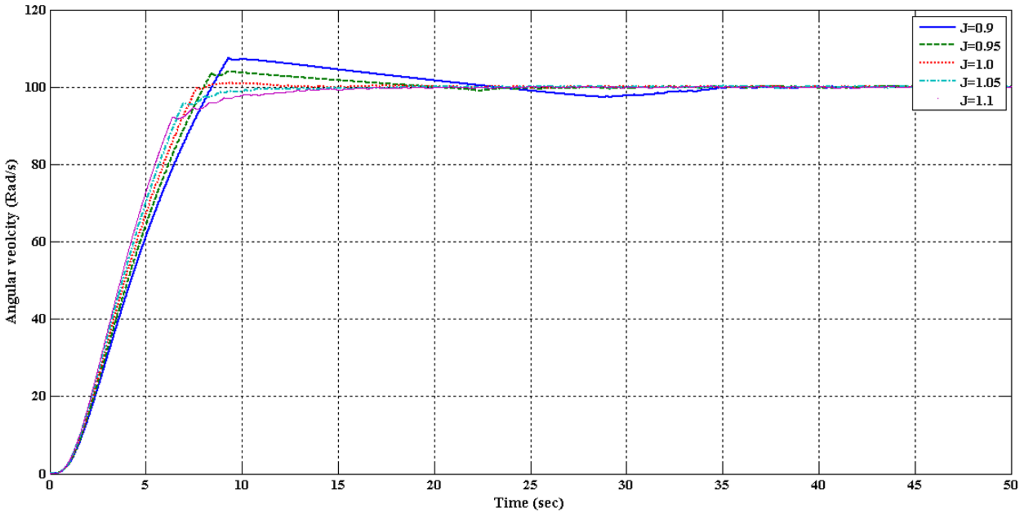

Figure 7. Response of angular velocity (PP and boost converter)

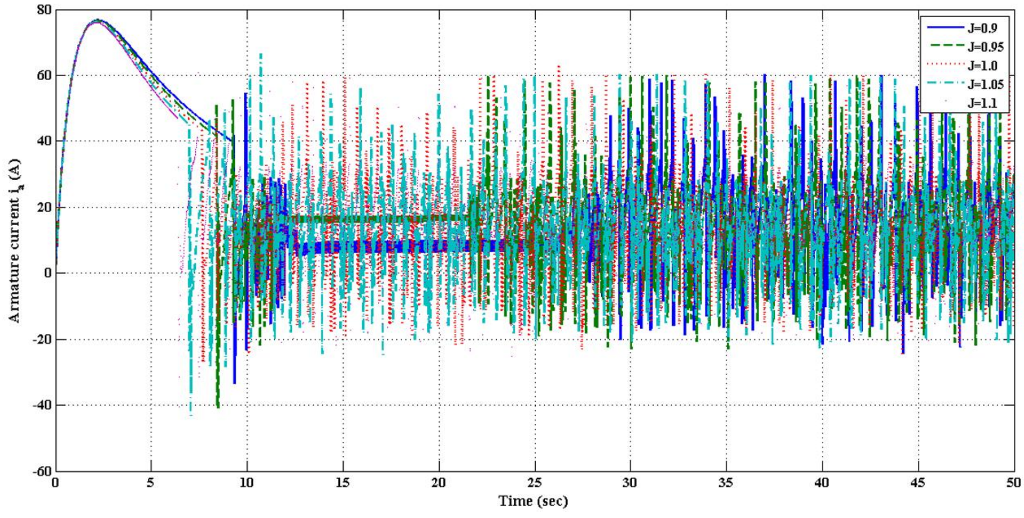

Figure 8. Response of armature current (PP and boost converter)

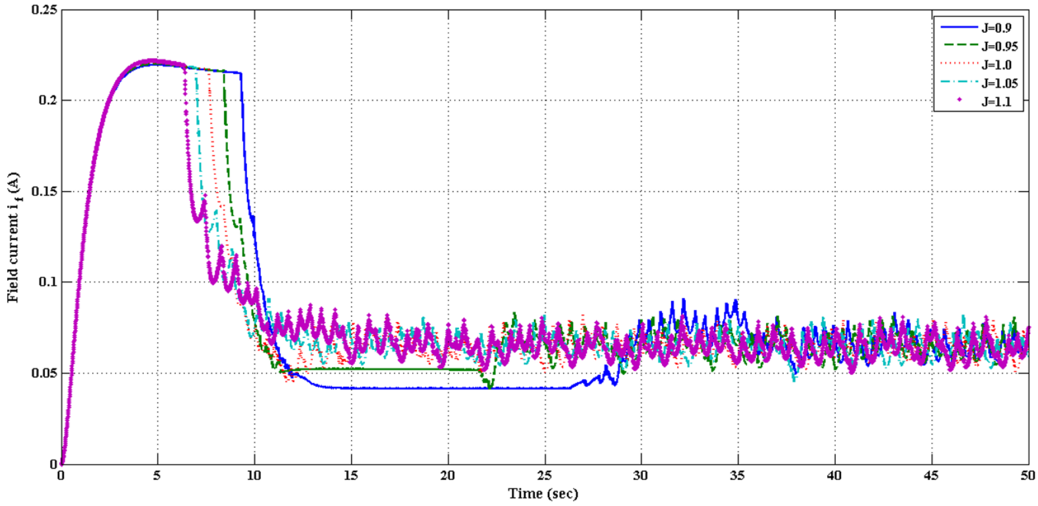

Figure 9. Response of field current (PP and boost converter)

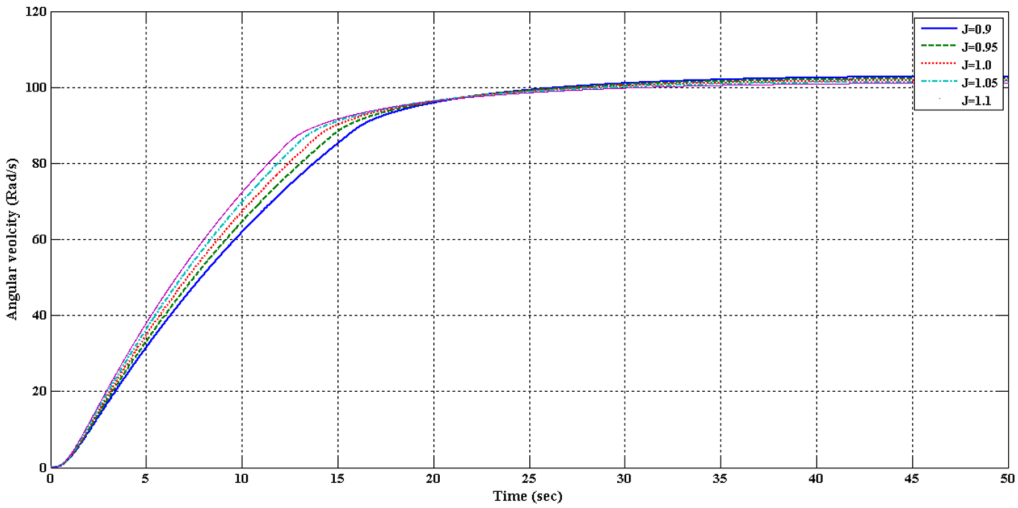

Figure 10. Response of angular velocity (PI and boost converter)

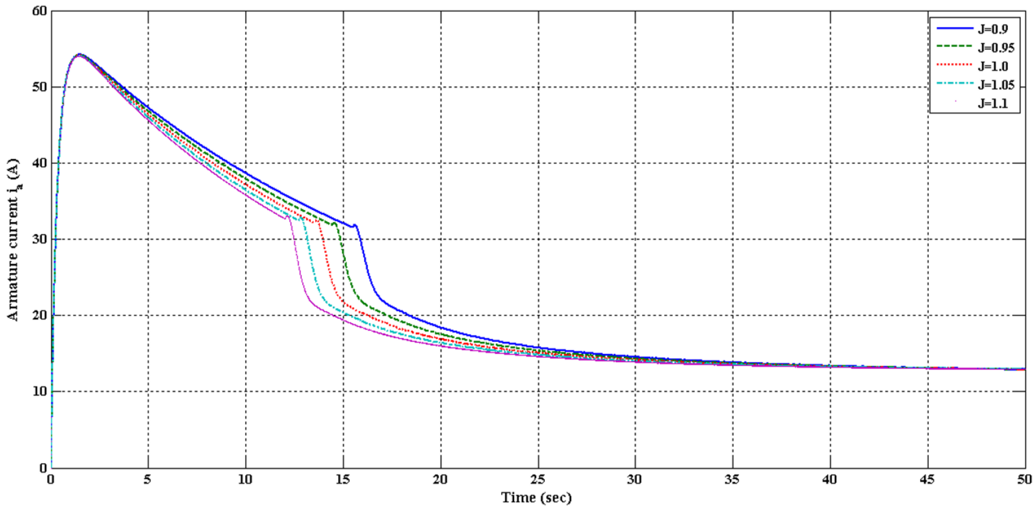

Figure 11. Response of armature current (PI and boost converter)

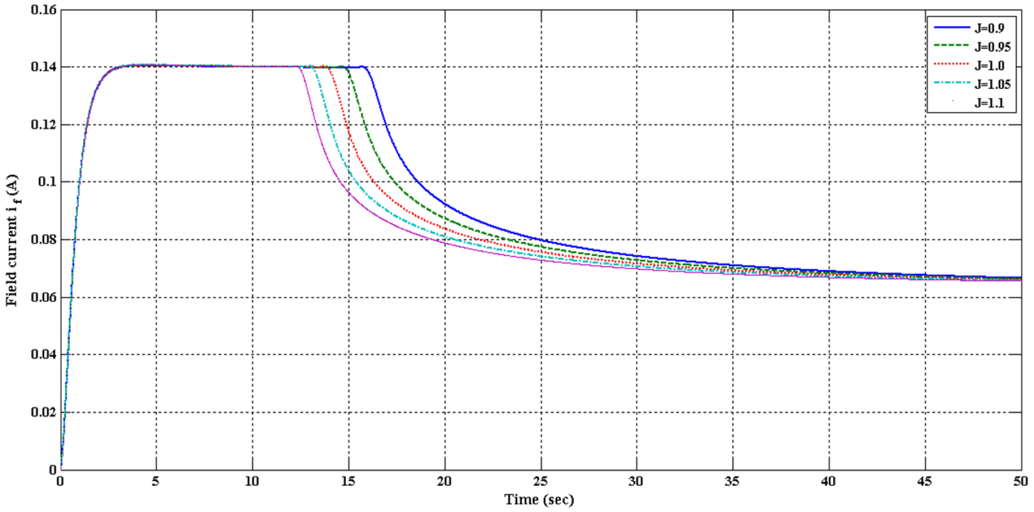

Figure 12. Time response of field current (PI and boost converter)

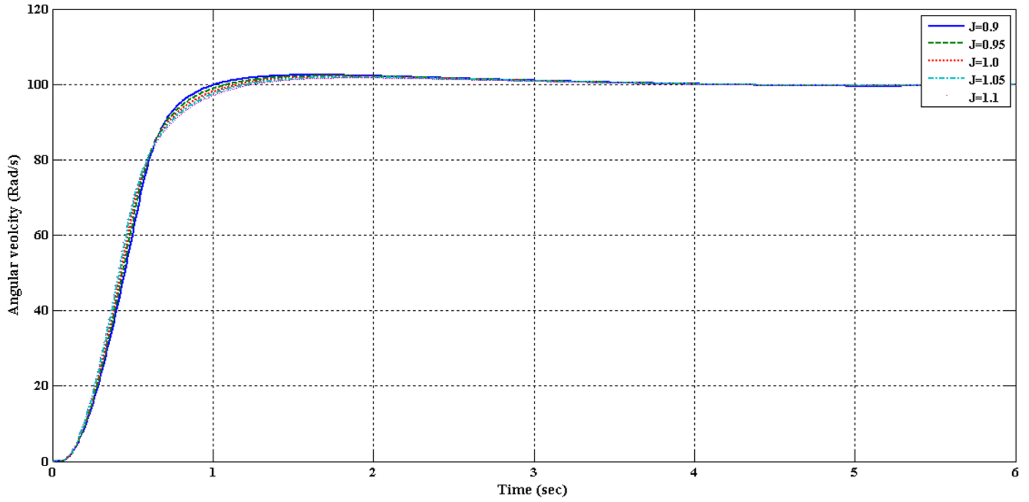

Figure 13. Response of angular velocity (PP and buck converter)

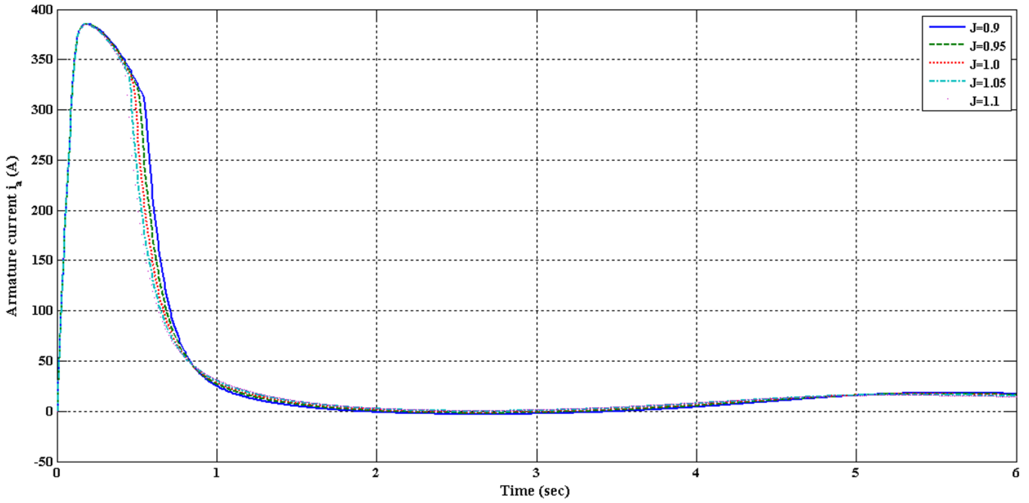

Figure 14. Response of armature current (PP and buck converter)

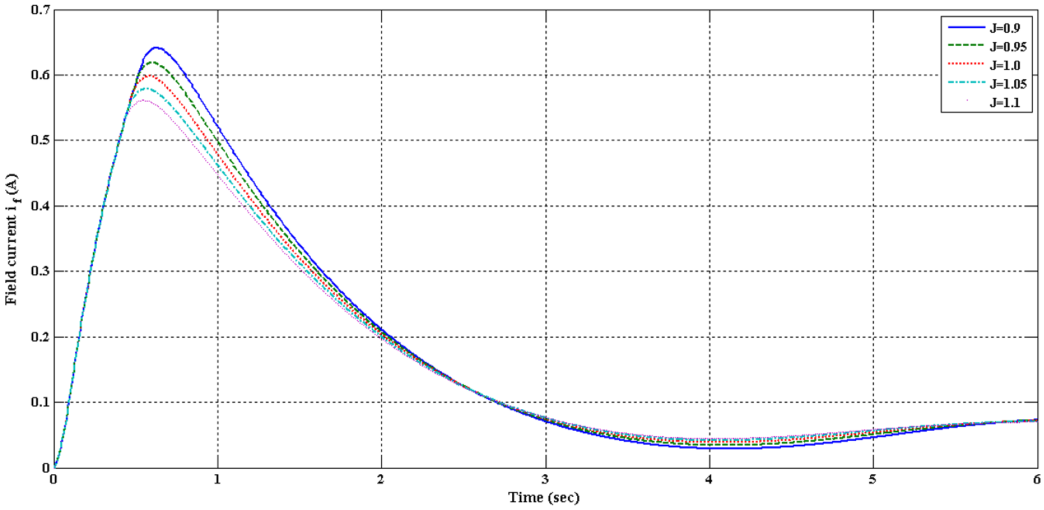

Figure 15. Response of field current (PP and buck converter)

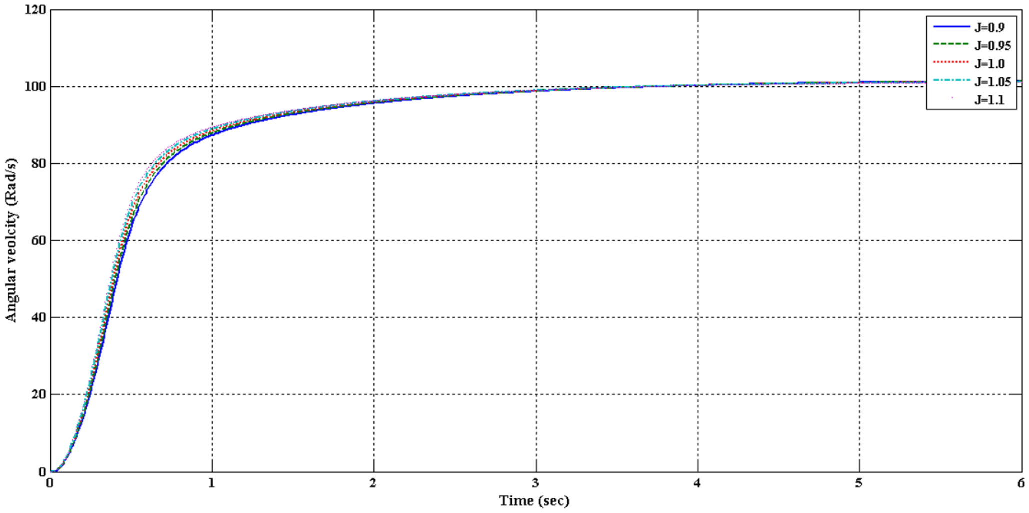

Figure 16. Response of angular velocity (PI and buck converter)

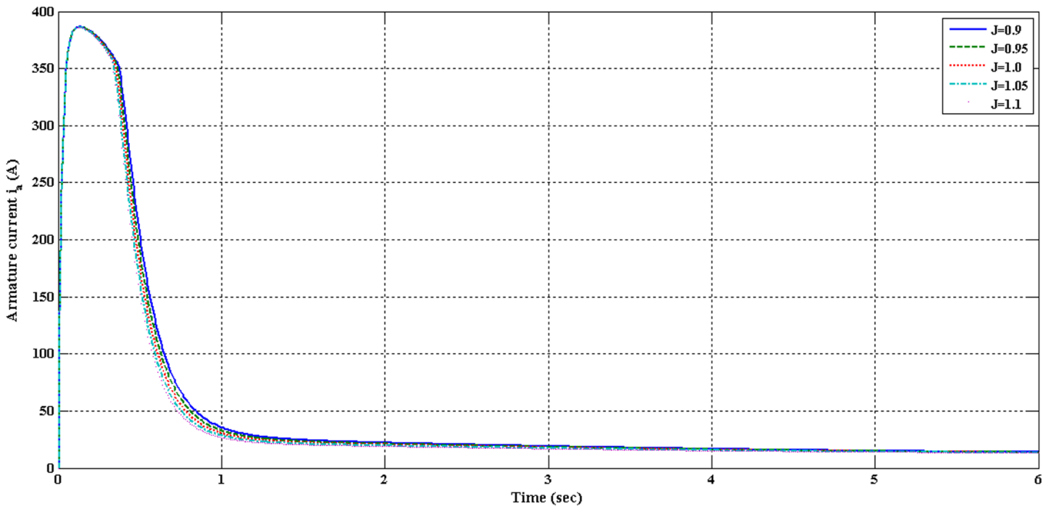

Figure 17. Response of rotor current (PI and buck converter)

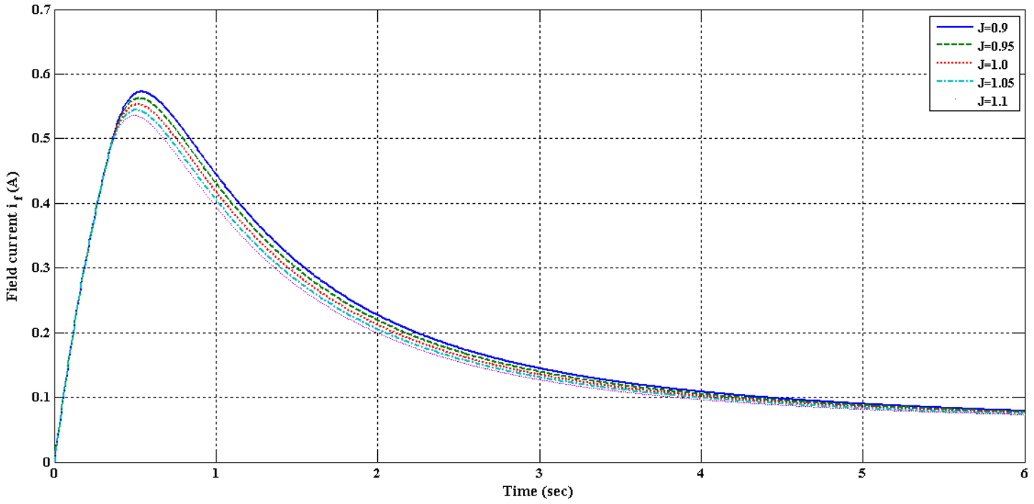

Figure 18. Response of excitation current (PI and buck converter)

Table 2. Time parameters of the two controllers

Parameter/controller	Pole placement	Proportional integral
t_r	0.85 s	1.7 s
e_{SS}	0.28% at J=0.9	1.33% at J=0.9

4. CONCLUSION

This study developed an improved structure for speed tracking control of nonlinear SWDCMs functioning with uncertainty. The proposed linear PP controller effectively improved the transient characteristics of motor angular velocity. DC/DC converter models were introduced in the design to drive the DC motor. The uncertainty in the inertia parameter of SWDCM was overcome by applying the proposed method. The simulation results demonstrated the effectiveness and application scope of the proposed technique.

REFERENCES

[1] S. D. Umans, *Fitzgerald and kingsley's electric machinery*, McGraw-Hil., vol. 319, no. 4. 2014.

[2] E. L. Cantor, G. A. Ramos, M. A. Ríos, and A. Albarracín, "Allocation of active power filter in DC traction systems," *International Transactions on Electrical Energy Systems*, vol. 23, no. 7, pp. 1191–1204, 2013, doi: 10.1002/etep.1651.

[3] P. Pany, R. K. Singh, and R. K. Tripathi, "Active load current sharing in fuel cell and battery fed DC motor drive for electric vehicle application," *Energy Conversion and Management*, vol. 122, pp. 195–206, Aug. 2016, doi: 10.1016/j.enconman.2016.05.062.

[4] F. Beltran-Carbajal, R. Tapia-Olvera, O. Aguilar-Mejia, A. Favela-Contreras, and I. Lopez-Garcia, "An online algebraic estimation approach of parameters and variable mechanical torque in shunt DC motors," *International Transactions on Electrical Energy Systems*, vol. 28, no. 1, pp. 1–22, Jan. 2018, doi: 10.1002/etep.2474.

[5] S. K. Valluru and M. Singh, "Trajectory control of DC shunt motor by NARMA Level-2 neuro controller," in *2016 IEEE 1st International Conference on Power Electronics, Intelligent Control and Energy Systems (ICPEICES)*, Jul. 2016, pp. 1–6, doi: 10.1109/ICPEICES.2016.7853600.

[6] A. Tepljakov, E. A. Gonzalez, E. Petlenkov, J. Belikov, C. A. Monje, and I. Petráš, "Incorporation of fractional-order dynamics into an existing PI/PID DC motor control loop," *ISA Transactions*, vol. 60, pp. 262–273, 2016, doi: 10.1016/j.isatra.2015.11.012.

[7] F. Beltran-Carbajal, R. Tapia-Olvera, I. Lopez-Garcia, and D. Guillen, "Adaptive dynamical tracking control under uncertainty of shunt DC motors," *Electric Power Systems Research*, vol. 164, pp. 70–78, 2018, doi: 10.1016/j.epsr.2018.07.033.

[8] S. Jayaprakash, "Comparison of solar based closed loop DC-DC converter using PID and fuzzy logic control for shunt motor drive," in *Proceedings-NCET NRES EM 2014: 2nd IEEE National Conference on Emerging Trends in New and Renewable Energy Sources and Energy Management*, 2015, pp. 115–117, doi: 10.1109/NCETNRESEM.2014.7088750.

[9] W. R. Abdul-Adheem, N. A. Shalash, and A. J. Ghaffoori, "Optimal full state feedback controller for two DC motor configurations with buck chopper," *Eurasian Journal of Analytical Chemistry*, vol. 13, no. 3, pp. 278–285, 2018.

[10] K. Sedghisigarchi, A. Hasanovic, A. Feliachi, and A. Davari, "Evaluation of three algorithms for nonlinear control of a DC shunt motor," in *Proc. of the Annual Southeastern Symposium on System Theory*, 2001, pp. 407–411, doi: 10.1109/SSST.2001.918555.

[11] R. Kumar, A. Choudhary, and S. L. Shimi, "Smooth starter for DC shunt motor using buck-boost power converter," in *Int. Conf. on Innovations in Control, Communication and Information Systems*, Aug. 2017, pp. 1–8, doi: 10.1109/ICICCIS.2017.8660830.

[12] S. M. Girirajkumar, A. A. Kumar, and N. Anantharaman, "Speed control of a real time D.C. shunt motor using SA based tuning of a PID controller," *International Journal of Computer Applications*, vol. 5, no. 11, pp. 20–26, 2010, doi: 10.5120/954-1331.

[13] N. A. Shalash and Y. N. Lafta, "PSS/E based placement wind/PV hybrid system to improve stability of Iraqi grid," *International Journal of Electrical and Computer Engineering (IJECE)*, vol. 10, no. 1, pp. 91–104, 2020, doi: 10.11591/ijece.v10i1.pp91-104.

[14] M. Veerachary, “Analysis of minimum-phase fourth-order buck DC-DC converter,” *IEEE Transactions on Industrial Electronics*, vol. 63, no. 1, pp. 144–154, Jan. 2016, doi: 10.1109/TIE.2015.2472525.

[15] A. S. Jaber and A. Z. Ahmad, “A new improvement of conventional PI/PD controllers for load frequency control with scaled fuzzy controller,” *International Journal of Engineering and Applied Sciences (IJEAS)*, vol. 2, no. 4, pp. 69–74, 2015.

[16] A. S. Jaber, A. Z. Ahmad, and A. N. Abdalla, “A new load frequency controller based on parallelization of fuzzy PD with conventional PI(FPD-PI),” 2014.

[17] K. C. Woo, J. M. Oh, and B. Do Yang, “DC-DC buck converter using analog coarse-fine self-tracking zero-current detection scheme,” *IEEE Transactions on Circuits and Systems II: Express Briefs*, vol. 66, no. 11, pp. 1850–1854, Nov. 2019, doi: 10.1109/TCSII.2018.2890267.

[18] T. Guo, Z. Wang, X. Wang, S. Li, and Q. Li, “A simple control approach for buck converters with current-constrained technique,” *IEEE Transactions on Control Systems Technology*, vol. 27, no. 1, pp. 418–425, Jan. 2019, doi: 10.1109/TCST.2017.2758347.

[19] A. Mamizadeh, N. Genc, and R. Rajabioun, “Optimal tuning of PI controller for boost DC-DC converters based on cuckoo optimization algorithm,” in *7th International IEEE Conference on Renewable Energy Research and Applications, ICRERA 2018*, Dec. 2018, pp. 677–680, doi: 10.1109/ICRERA.2018.8566883.

[20] M. H. B. Nozadian, E. Babaei, and V. Ranjbarzad, “Steady state analysis of dual switched boost inverter,” in *Proceedings-2018 IEEE 12th International Conference on Compatibility, Power Electronics and Power Engineering, CPE-POWERENG 2018*, Jun. 2018, pp. 1–6, doi: 10.1109/CPE.2018.8372572.

[21] A. Tiwari, O. Jaga, and S. S. Soni, “Sliding mode controller based interleaved boost converter for fuel cell system,” in *2017 Recent Developments in Control, Automation and Power Engineering, RDCAPE 2017*, May 2018, pp. 516–520, doi: 10.1109/RDCAPE.2017.8358325.

[22] Y. Sharma, “DC shunt motor speed control and analysis using ziegler-nichols algorithm with PID controller,” *International Journal of Modern Trends in Engineering and Research*, vol. 2, no. 7, pp. 89–97, 2015.

[23] S. Malek, “A new nonlinear controller for DC-DC boost converter fed dc motor,” *International Journal of Power Electronics*, vol. 7, no. 1–2, pp. 54–71, 2015, doi: 10.1504/IJPELEC.2015.071199.

[24] W. R. Abdul-Adheem, “Design and simulation of a normalized fuzzy logic controller for the quadruple-tank process,” *Indonesian Journal of Electrical Engineering and Computer Science*, vol. 18, no. 1, pp. 227–234, Apr. 2020, doi: 10.11591/ijeecs.v18.i1.pp227-234.

[25] W. R. Abdul-Adheem, “An enhanced particle swarm optimization algorithm,” *International Journal of Electrical and Computer Engineering (IJECE)*, vol. 9, no. 6, pp. 4904–4907, Dec. 2019, doi: 10.11591/ijece.v9i6.pp4904-4907.

BIOGRAPHIES OF AUTHORS

Nadheer Abdulridha Shalash received the B.S. degree in 2003, the M.S. degree in 2008 from the University of Technology-Iraq. The Ph.D. degree in Electrical Power Engineering/University Malaysia Pahang in 2015. Research interests include power systems, power converters, and optimization. Email: nadheer.a.shalash@almamonuc.edu.iq.

Wameedh Riyadh Abdul-Adheem received the B.Sc. degree (with highest honors) in Electrical Engineering from the University of Baghdad at Baghdad in 1998, and he received the M.Sc. degree in Computer and Control Engineering from the University of Baghdad at Baghdad in 2001, and Ph.D. degree in computer and control engineering at the University of Baghdad at Baghdad in 2019. His research interests include signal processing, nonlinear control, and optimization. Email: wameedh.r.abduladheem@almamonuc.edu.iq.

Yasir K. Abdul Jabbar Assistant Lecturer at Electrical Power Techniques Engineering Department, Al-Ma’moon University College. M.Sc. In Electrical Engineering/ Computer and Control from Baghdad University. Research interest in control theory, system identification and robotics. Email: yasir.k.abduljabbar@almamonuc.edu.iq.